Eu^{3+} luminescence in Eu-doped $KMgF_3$ crystals investigated by site-selective laser-excitation spectroscopy

Hyo Jin Seo,[1,*] Taiju Tsuboi,[2] and Kiwan Jang[3]
[1]*Department of Physics, Pukyong National University, Pusan 608-737, Republic of Korea*
[2]*Faculty of Engineering, Kyoto Sangyo University, Kamigamo, Kita-ku, Kyoto 603-8555, Japan*
[3]*Department of Physics, Changwon National University, Changwon 641-773, Republic of Korea*
(Received 28 May 2004; published 11 November 2004)

Luminescence properties of Eu^{3+} ions in $KMgF_3$ are investigated by site-selective laser-excitation spectroscopy. Two different types of Eu^{3+} centers are identified in $KMgF_3$:Eu^{3+} (0.01 mol %). Two lines at 570.16 and 573.87 nm corresponding to two Eu^{3+} centers are observed in the excitation spectrum of the $^7F_0 \rightarrow {}^5D_0$ transition. The former line is much stronger than the latter line. The dominant Eu^{3+} center is due to the isolated Eu^{3+}-V_c (charge-compensating vacancies) pair and the other Eu^{3+} centers are attributable to a clustering of Eu^{3+}-V_c pairs. At high concentration of Eu ions (above 0.5 mol %), new excitation lines due to clustering of Eu^{3+}-V_c pairs appear in the excitation spectra of the $^7F_0 \rightarrow {}^5D_0$ transition. Luminescence from most of the Eu^{3+} centers is quenched as the temperature is raised to 305 K. Such a luminescence quenching is explained by an energy transfer from Eu^{3+} to an H center formed in the vicinity of Eu^{3+}-V_c pair.

DOI: 10.1103/PhysRevB.70.205113 PACS number(s): 78.60.−b, 32.50.+d, 78.55.Fv

I. INTRODUCTION

When rare-earth (RE) ions are introduced into host materials, they may substitute for cation sites. If the valence state of the rare-earth ions is different from that of the cation ions, anion or cation vacancies are formed for charge compensation. The charge-compensating vacancies are expected to locate in the vicinity of the rare-earth ions. The different positions of the vacancies relative to the rare-earth ions give rise to different types of rare-earth centers. In addition to the isolated rare-earth ions with the vacancies, clustering of such rare-earth ions occurs, resulting in the presence of various cluster configurations in the host materials such as alkali-metal halides and alkaline-earth halides.[1–6]

Optical properties of rare-earth-doped $KMgF_3$ have been extensively investigated not only for the purpose of scientific interest, but also from the practical viewpoint of UV scintillators[7] and radiation dosimetry.[8,9] Divalent europium and samarium ions substitute for K^+ ions at the sites with cubic (O_h) and three different noncubic (C_{4V}, C_{2V}, and C_{3V}) symmetries depending on the location of charge-compensating K^+-ion vacancies in $KMgF_3$.[10–14] Doping of $KMgF_3$ by trivalent rare-earth ions is expected to cause quite a different situation from the case of doping by divalent rare-earth ions because RE^{3+} has different charge-compensating vacancies and ionic radius from the case of RE^{2+}. No detailed study has been done on the defect structure of trivalent rare-earth-doped $KMgF_3$, although various investigations on the trivalent rare-earth-doped $KMgF_3$ by ESR (Refs. 15–17) and optical spectroscopy[9,18,19] have been reported. Luminescence properties of Ce^{3+} in $KMgF_3$ were investigated by Francini *et al.*[18] and Martini *et al.*[9] They suggested that a Ce^{3+} ion substitutes for a K^+ site and there exist two different Ce^{3+} centers causing the two luminescence bands. Francini *et al.* attributed the two centers to the unperturbed (cubic) site and a site perturbed (noncubic) by two K^+-ion vacancies, while Martini *et al.* suggested that they are ascribed to the isolated Ce^{3+} ions and complex centers formed by aggregation of Ce^{3+} ions.

Among rare-earth ions, europium can be stabilized in a divalent or trivalent state depending on the chemical composition of the host. In the Eu-doped $KMgF_3$, divalent europium is certainly observed by absorption and luminescence spectroscopy and there are many detailed reports on the optical properties of Eu^{2+} in $KMgF_3$.[10–14] Only a few works have been published on Eu^{3+} luminescence in $KMgF_3$:Eu. Shiran *et al.*[20] reported narrow Eu^{3+} emission bands in the region of 520–630 nm, and Merkle *et al.*[21] observed weak luminescence lines which seem to be due to Eu^{3+} in $KMgF_3$. Sommerdijk and Bril[22] reported the Eu^{3+} emission line due to the $^5D_0 \rightarrow {}^7F_0$ transition at 578.0 nm in $KMgF_3$. However, no figure was presented to show the experimental results in their paper. To our knowledge, no report has been given in detail so far regarding the Eu^{3+} luminescence spectra and the characteristics of the Eu^{3+} ion in $KMgF_3$ crystal.

We used site-selective laser-excitation spectroscopy to investigate substitution sites for Eu^{3+} and the defect structure of the trivalent europium-ion-doped $KMgF_3$ crystals. The narrow $4f \rightarrow 4f$ transitions characteristic of trivalent europium in $KMgF_3$ offer a convenient method for directly monitoring the different sites. Eu^{3+} has a simple multiplet pattern of its energy level, which makes this ion particularly suited as a probe of local structure.[23,24] Since each Eu^{3+} center with different crystal-field symmetry possesses a unique optical transition in the $^7F_0 \rightarrow {}^5D_0$ excitation spectrum, the evolution of the cluster sites can be reliably followed as a function of doping concentration of Eu^{3+} ions. In this paper, we show that there exist two different types of Eu^{3+} centers, isolated Eu^{3+}-V_c pairs, and clusters of Eu^{3+}-V_c pairs.

II. EXPERIMENTAL PROCEDURE

Single crystals of $KMgF_3$ doped with europium ions were grown from the melt in Ar-gas atmosphere by the Czochralski method at Pukyong National University. The concentrations of europium ions were 0.01, 0.5, and 2.5 mol % in the melt. For comparison with the experimental results on our crystals, we took the same measurements on a $KMgF_3$:Eu (0.25 mol %) crystal grown by the Stockbarger method at Changwon National University and obtained nearly the same results as the results of our sample (0.5 mol % Eu-doped $KMgF_3$). This indicates that the luminescence properties of Eu^{3+} investigated in our $KMgF_3$ are not dependent on the individual crystal samples.

Annealing and quenching experiments were taken on the samples at argon gas atmosphere. The samples were heated up to 700 °C, kept at this temperature for 5 h, and then quenched down to room temperature by letting it cool down in the platinum boat in which it was heated. The excitation source was a dye laser (Spectron Laser Sys. SL4000) pumped by the second harmonic (532 nm) of a pulsed Nd:YAG (yttrium aluminum garnet) laser (Spectron Laser Sys. SL802G). The laser beam was focused inside the sample with a cross-sectional area of about 3 mm^2. The pulse energy was about 5 mJ with a 10 Hz repetition rate and 5 ns duration. A 355-nm pulsed laser with about 7-mJ pulse energy was used for UV irradiation on the samples. The beam path of the 355-nm laser beam coincided with that of the excitation laser beam on the samples. The samples were placed in a liquid- helium flow cryostat for measurements in the variable-temperature region (10–305 K). The luminescence was dispersed by a 75-cm monochromator (Acton Research Corp. Pro-750) and observed with a photomultiplier tube (PMT) (Hamamatsu R928) with which the signal is detectable up to about 850 nm. The excitation spectra for the $^7F_0 \rightarrow {}^5D_0$ transition were obtained by monitoring total luminescence detecting with the monochromator in zero order of diffraction. Suitable filters were used to eliminate the intense scattering peaks in the spectrum due to the scattered laser irradiation. The slit widths of the monochromator were normally set to give a resolution of 0.025 nm for emission spectra.

III. RESULTS

The presence of Eu^{2+} ions in our Eu-doped $KMgF_3$ crystals was confirmed by means of absorption and two-photon excitation spectroscopy. Eu^{2+} absorption bands were the same as those observed by Tsuboi and Scacco.[12] The parity forbidden $4f^7 \rightarrow 4f^7$ transition of Eu^{2+} was investigated by two-photon excitation spectroscopy and the results were published in Ref. 10.

Figure 1 shows the excitation spectrum corresponding to the $^7F_0 \rightarrow {}^5D_0$ transition at 10 K for the sample with Eu concentration of 0.01 mol %. Two excitation lines (labeled *A* and *B*) are observed in the spectrum. No other line was detected in the temperature range 10–305 K. The dominant excitation line is at 570.16 nm (*A*) and the weak line at 573.87 nm (*B*). Each line appearing in the spectrum corresponds to a different Eu^{3+} center since the transition between the nondegenerate $^7F_0 \rightarrow {}^5D_0$ levels can have only one line per site. We will call the Eu^{3+} ion that gives rise to the *A* excitation line site *A* hereafter. The position of the dominant

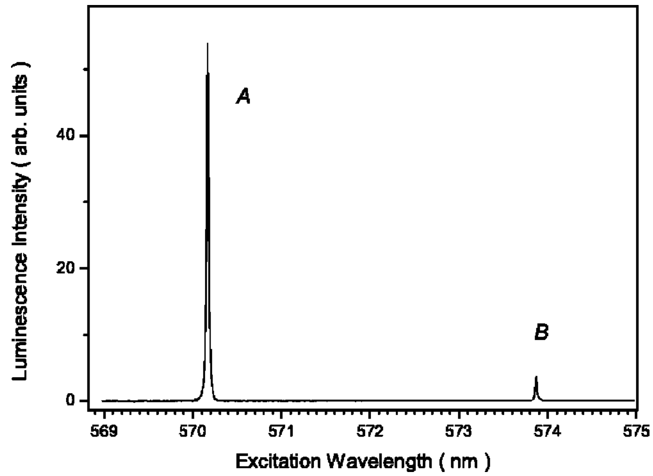

FIG. 1. Excitation spectrum for the $^7F_0 \rightarrow {}^5D_0$ transition of Eu^{3+} in the $KMgF_3$ crystal (sample I: Eu concentration of 0.01 mol %). The spectrum was obtained by monitoring the luminescence due to the $^5D_0 \rightarrow {}^7F_J$ $(J=0,1,2,\ldots,6)$ transitions in the 560–800 nm region in $KMgF_3$ at 10 K. The peaks are labeled by *A* and *B*.

line (570.16 nm) in $KMgF_3$:Eu^{3+} is similar to that of the $CsMgF_3$:Eu^{3+} (568.1 nm) and $RbMgF_3$:Eu^{3+} (569.1 nm),[22] in which monovalent ions (K^+, Cs^+, and Rb^+) are surrounded by 12 F^- ions in these crystals.

Figures 2 and 3 show the emission spectra of the $^5D_0 \rightarrow {}^7F_J$ $(J=1,2,\ldots,5)$ transitions from the individual Eu^{3+} center obtained by tuning the laser to resonance with each excitation line in Fig. 1. Emission lines for the $^5D_0 \rightarrow {}^7F_6$ transition are expected to appear at longer wavelengths than 800 nm, but they were not observed, presumably because they were too weak. As observed in usual crystals containing Eu^{3+} ions, the $^5D_0 \rightarrow {}^7F_2$ luminescence intensity is stronger than the other $^5D_0 \rightarrow {}^7F_j$ luminescence. Each Eu^{3+} center exhibits numerous emission lines between 12 500 and 17 500 cm^{-1} originating from the $^5D_0$ level. The energy levels of $^5D_0$ and ^5F_J $(J=1,2,\ldots,5)$ multiplets of the two Eu^{3+} centers (sites *A* and *B*) were identified from the emission and excitation spectra. The transitions between $^5D_0$ and ^7F_J and energy levels are given in Tables I and II, respectively.

Figure 4 shows the excitation spectra corresponding to the $^7F_0 \rightarrow {}^5D_0$ transition for three $KMgF_3$ crystals with different Eu concentrations at 10 K. We refer to samples doped with Eu concentrations of 0.01, 0.5, and 2.5 mol % as sample I, sample II, and sample III, respectively. With increasing Eu concentration, the excitation lines (*A* and *B*) are broadened and the peak height of line *B* relative to line *A* is increased. The ratio of the peak height of line *B* to that of line *A* was estimated to be 1.6 times larger for sample II than for sample I, and the ratio is much larger (6.4 times) for sample III. The bandwidth of line *A* of sample I is estimated to be 0.92 cm^{-1} and the line is broadened by 2.2 cm^{-1} (sample II) and 5.1 cm^{-1} (sample III) [see Fig. 4(b)]. New excitation lines, which are not observed for sample I, appear in the enlargement of the excitation spectrum for sample II, although their peaks are very weak, as shown in Fig. 5. The relative intensities of these lines are increased for sample III, but the lines are overlapped by broad and strong lines *A* and *B*. The peaks

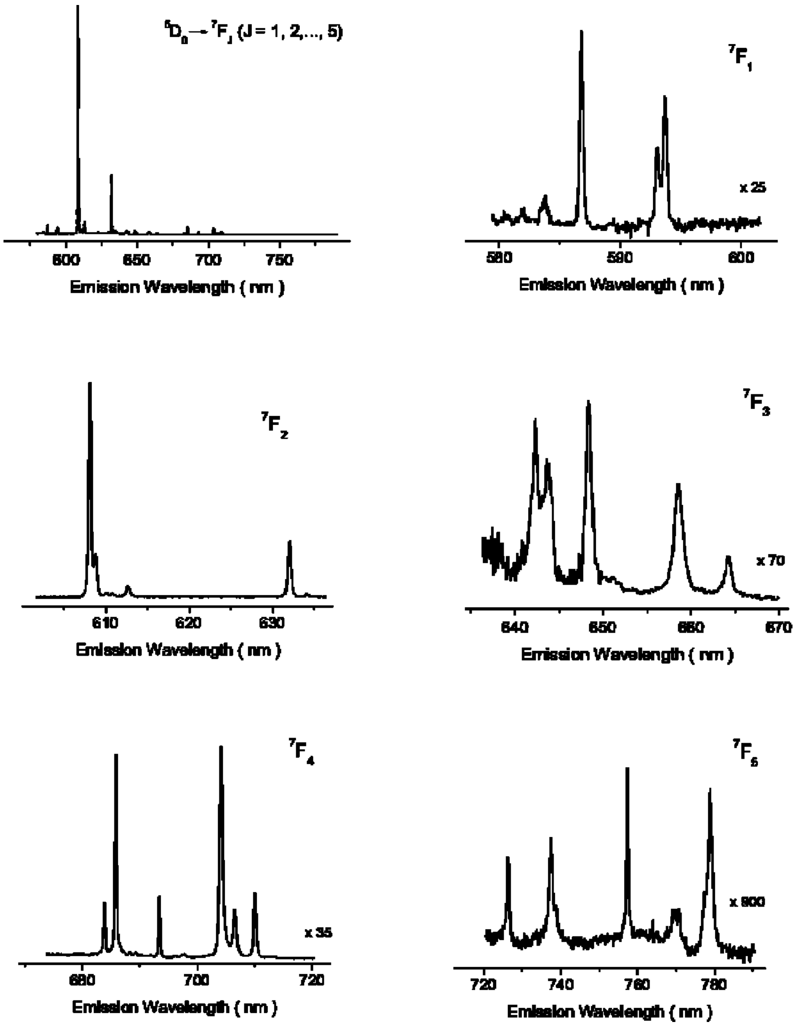

FIG. 2. $^5D_0 \rightarrow {}^7F_J$ $(J=0,1,2,\ldots,5)$ emission spectrum for site *A* exciting at 570.16 nm in $^5D_0$ at 10 K.

are labeled by *C*, *D*, *E*, *F*, *G*, *H*, *I*, and *J*, as indicated in Fig. 5. Relatively intense but broad lines are observed at 566.39 (*D*) and 567.74 nm (*E*). Additionally, several weak lines are at 564.36 nm (*C*), 568.45 nm (*F*), 569.43 nm (*G*), 571.40 nm (*H*), 573.30 nm (*I*), and 575.51 nm (*J*). Each line (except for the phonon side band) appearing in the spectrum corresponds to a different Eu^{3+} center.

Figure 6 shows the 10 K emission spectra of the $^5D_0 \rightarrow {}^7F_J$ $(J=0,1,2)$ transitions from individual sites obtained by tuning the laser to resonance with each excitation line in Fig. 5. The emission spectra should be different from each other if all the excitation lines are responsible for the different Eu^{3+} centers. However, the emissions obtained by exciting at some excitation lines show the same spectral and temporal behaviors. The same emission profiles are observed for the spectra obtained by irradiation with the *E*, *F*, and *A* excitation lines. The emission spectrum obtained by irradiation with the *C* excitation line consists of the spectrum obtained by irradiation with the *D* excitation line and the spectrum obtained by irradiation with the *A* excitation line. Two excitation lines (called C_A and C_D lines) are superimposed at the broad *C* excitation lines. From these results, we identify that the *E*, *F*, and C_A lines are phonon side bands associated with the main sharp *A* line [zero phonon line (ZPL) *A*], while the C_D phonon side bands are associated with the zero phonon line *C*. These are also confirmed by the appearance of the zero phonon line at 570.16 nm for the site *A* in each emission spectrum (see the left side of Fig. 6). The observed phonon side bands are at 53 cm^{-1} (*E*), 75 cm^{-1} (*F*), and 172 cm^{-1} (C_A) from the zero phonon line *A* and at 55 cm^{-1} (C_D) from the zero phonon line *D*. As a result, there are seven measurable Eu^{3+} centers (i.e., the sites *A*, *B*, *D*, *G*, *H*, *I*, and *J*) in 0.5 mol % Eu-doped $KMgF_3$ at 10 K.

Figure 7(a) shows the excitation spectrum of the $^7F_0 \rightarrow {}^5D_0$ transition for the sample irradiated by a 355 nm pulsed laser at 10 K. In addition to the lines *A* and *B*, new broadband peaking at 571.7 nm appears with a weak band at 573.3 nm. The intensity of these new bands increases by increasing 355 nm pulsed laser output and irradiation time and is weaker for the sample with low Eu concentration. When the 355-nm-irradiated sample was heated to room temperature, the new bands completely disappeared in the excitation spectrum measured at 10 K. We attribute the new bands to the Eu^{3+} centers due to the formation of $[F_2^-]$ centers near the Eu^{3+}-V_c which is discussed in Sec. IV. The emission spectrum of the $^5D_0 \rightarrow {}^7F_J$ transitions obtained by exciting at 571.7 nm is shown in Fig. 7(b). The most intense luminescence line of the $^5D_0 \rightarrow {}^7F_2$ transition is observed at 633.8 nm, which is quite different from those for the sites *A* and *B*, in which the strongest lines of the $^5D_0 \rightarrow {}^7F_2$ transi-

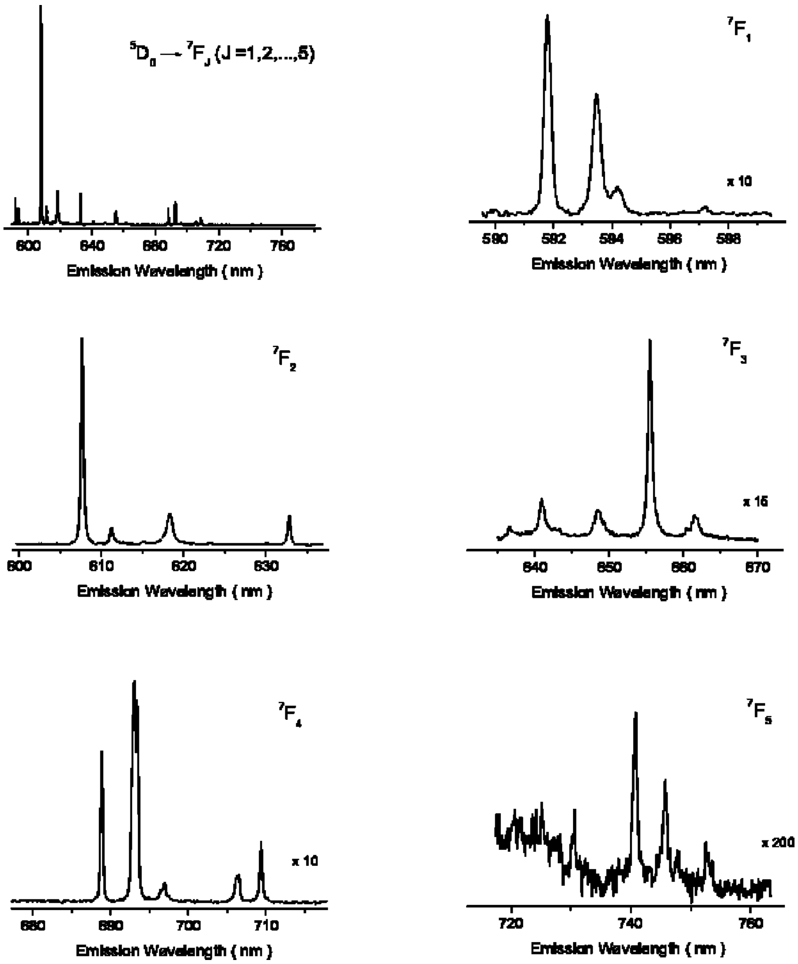

FIG. 3. $^5D_0 \rightarrow {}^7F_J$ $(J=0,1,2,\ldots,5)$ emission spectrum for site *B* exciting at 573.87 nm in $^5D_0$ at 10 K.

tions are around 610 nm. The decay of the $^5D_0$ level was single exponential with a lifetime of 790 μs.

The excitation spectra of the $^7F_0 \rightarrow {}^5D_0$ transition for different crystal temperatures are displayed in Fig. 8. The luminescence intensities of all the lines decrease rapidly above a certain temperature with increasing temperatures. The lines *B* and *D* disappear in the spectra obtained at 150 and 220 K, respectively. The intensity of the luminescence from the site *A* drastically decreases with increasing temperature, but it is still detectable even at 305 K. The *A* excitation line shifts about 4 cm^{-1} to lower energy with increasing temperature from 10 K to 300 K, as shown in the inset of Fig. 8. A new line (called *K*) appears at 569.82 nm above 260 K and its peak becomes higher than the peak of line *A* at room temperature. The *K* line may be hidden under the intense *A* line at low temperature. The *K* line was also observed in the excitation spectrum for sample III and the intensity ratio of the excitation lines between sites *K* and *A* is the same as that of sample II. This indicates that site *K* is not due to the cubic-site Eu^{3+} as discussed in Sec. IV. We note that only three excitation lines (*K*, *A*, and *I*) are observed at room temperature.

The decay times of the $^5D_0$ luminescence of all the sites were measured in the temperature range from 10 to 305 K. The decay times for the two major sites *A* and *B* are estimated to be 616 and 470 μs, and those for the minority sites *D*, *G*, *H*, *I*, and *J* are 394, 636, 644, 810, and 787 μs, respectively, at 10 K and 1.5 ms for site *K* at room temperature. Figure 9 plots lifetimes of the $^5D_0$ luminescence for sites *A*, *B*, *D*, and *I* as a function of temperature. We observe a quenching of decay times. The temperatures giving rise to the lifetime quenching are the same as the temperatures giving rise to the intensity quenching of the $^5D_0$ luminescence. The critical quenching temperatures are 60, 150, 210, 230, and 300 K for sites *D*, *A*, *C*, and *I*, respectively. The lifetimes for sites *G* and *H* are nearly constant up to about 120 K, but those were not measurable due to overlapping of those excitation lines with the broadened *A* excitation line above this temperature. It is noted that the site with shorter decay time tends to have lower quenching temperature, and site *K* with a much longer decay time of 1.5 ms exhibits no quenching up to 305 K.

IV. DISCUSSION

A Mg^{2+} ion forms an octahedron composed of six F^- ligands in $KMgF_3$. The K^+ ion has 12 F^- nearest neighbors with cuboctahedral O_h symmetry and is surrounded by eight $[MgF_6]^{-4}$ octahedrons. The small Mg^{2+} ion (ionic radius is 0.86 Å) bonds strongly with the F^- ligands in the $[MgF_6]^{-4}$ octahedron, while the large Eu-F distance in the $[KF_{12}]^{-11}$ cuboctahedron and the presence of the surrounding $[MgF_6]^{-4}$ octahedrons leads to low covalency between the K^+ ion (1.78 Å) F^-.[14] Consequently, the site environment of Mg^{2+} is

TABLE I. Observed transitions of Eu^{3+} for the sites *A* and *B* in $KMgF_3$ obtained from excitation and emission spectra at 10 K.

	Site *A*		Site *B*	
	nm	cm^{-1}	nm	cm^{-1}
$^7F_0 \rightarrow {}^5D_0$	570.16	17539	573.87	17426
$^5D_0 \rightarrow {}^7F_1$	586.81	17041	591.80	16898
	593.07	16861	593.49	16849
	593.72	16843	594.21	16829
$^5D_0 \rightarrow {}^7F_2$	608.12	16444	607.71	16455
	608.82	16425	611.27	16359
	612.70	16321	618.35	16172
	632.06	15821	623.85	16029
$^5D_0 \rightarrow {}^7F_3$	642.34	15568	636.59	15709
	643.74	15534	640.96	15602
	648.35	15424	648.54	15419
	658.55	15185	655.50	15256
	664.21	15055	661.64	15114
$^5D_0 \rightarrow {}^7F_4$	683.88	14622	688.86	14517
	685.89	14580	693.01	14430
	693.48	14420	693.44	14421
	704.17	14201	696.97	14348
	706.57	14153	706.40	14156
	710.10	14083	709.36	14097
$^5D_0 \rightarrow {}^7F_5$	726.32	13768	730.54	13689
	737.45	13560	740.72	13500
	757.40	13203	745.72	13410
	770.27	12982	747.86	13371
	778.93	12838	752.72	13285

TABLE II. Energies (in cm^{-1}) of the $^5D_0$ and ^7F_J levels of Eu^{3+} for the sites *A* and *B* in $KMgF_3$.

	Site *A*	Site *B*
$^7F_0$	0	0
$^7F_1$	498	528
	678	576
	696	596
$^7F_2$	1095	970
	1114	1066
	1218	1254
	1718	1624
$^7F_3$	1971	1717
	2005	1824
	2115	2014
	2354	2170
	2484	2312
$^7F_4$	2917	2909
	2959	2996
	3119	3005
	3338	3078
	3386	3269
	3456	3328
$^7F_5$	3771	3737
	3979	3925
	4336	4016
	4557	4052
	4701	4140
$^5D_0$	17539	17426

significantly different from that of K^+. Eu^{3+} has an ionic radius of 1.21 Å, which is much larger than Mg^{2+}. Therefore, it is reasonable to suggest that an Eu^{3+} ion preferentially substitutes for a larger K^+ ion (1.78 Å) as the case of Ce^{3+} ions (1.28 Å) in $KMgF_3$ suggested by Francini *et al.*[18] and Martini *et al.*[9]

The site symmetries of Eu^{3+} can be determined from the number of emission lines of the $^5D_0 \rightarrow {}^7F_J$ $(J=1,2,\ldots,6)$ transitions.[23] Theoretically, for example, the $^7F_1$ and $^7F_2$ multiplets split by crystal-field perturbation into two and four sublevels for the tetragonal site and three and five sublevels for the orthorhombic site. Induced electric dipole (ED) and magnetic dipole (MD) selection rules predict the permitted transitions between excited $^5D_0$ and ground ^7F_j levels of Eu^{3+}. The transitions between *J* sublevels are further restricted by symmetry selection rules.[23] In the case of $^5D_0 \rightarrow {}^7F_1$ and $^5D_0 \rightarrow {}^7F_2$ transitions of Eu^{3+} with tetragonal crystal-field symmetry, only two and two transition lines are allowed, respectively. It is known that the transitions between $^5D_0$ and ^7F_J (J=0, 1, and 2) states of Eu^{3+} or Sm^{2+} doped in fluoride crystals such as $LiYF_4{:}Eu^{3+}$ (Ref. 24) and $KMgF_3{:}Sm^{2+}$ (Ref. 11) strictly obey the induced ED and MD selection rules and the symmetry selection rules. By applying the selection rules to the transitions from $^5D_0$ to ^7F_j levels of Eu^{3+} in $KMgF_3$, we have found the sites *A* and *B* have lower symmetries belonging neither in tetragonal (C_{4V}) nor orthorhombic (C_{2V}) symmetries. We note that the tetragonal and orthorhombic sites for Eu^{2+} and Sm^{2+} are dominantly identified with cubic symmetry (O_h) in $KMgF_3{:}Eu^{2+}$ and $KMgF_3{:}Sm^{2+}$.[10,11,13]

The induced ED transition cannot occur when the point group of the site contains a center of symmetry (e.g., cubic symmetry) and the $^7F_0 \rightarrow {}^5D_0$ transition for the cubic site is further forbidden by the selection rules. The MD transition is allowed only from the $^7F_1$ level to the $^5D_0$ level in cubic symmetry. The $^7F_1$ levels of Eu^{3+} ions can be populated thermally by the $^7F_0$ levels at high temperature due to the small energy difference of about 550 cm^{-1}. To ascertain the presence of cubic-site Eu^{3+} in $KMgF_3$, we measured the excitation spectrum of the $^7F_1 \rightarrow {}^5D_0$ transition at temperatures higher than 150 K. However, no transition line from cubic-site Eu^{3+} was observed, but only the lines at 586.8 and 593.7 nm due to the site *A* were observed.

The substitution of Eu^{3+} for K^+ gives rise to two K^+-ion vacancies (V_c) close to Eu^{3+} forming an Eu^{3+}-V_c pair for charge compensation. The trivalent europium ion is more tightly bound to the vacancies than a divalent europium ion in $KMgF_3$ because two extra charges on the Eu^{3+} ion increase effectively the Coulomb attraction. The cubic-site

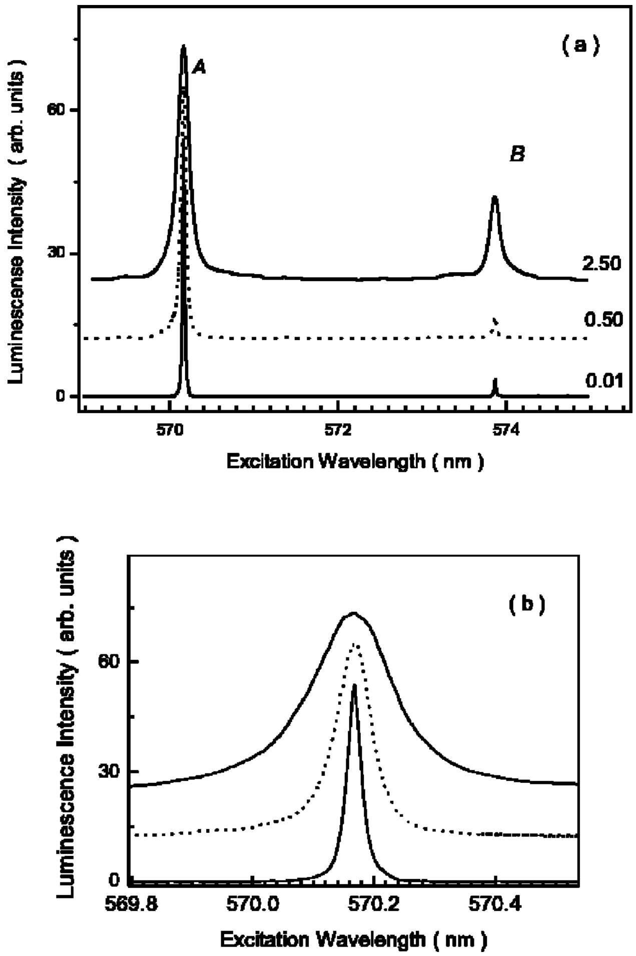

FIG. 4. (a) Excitation spectra for three different $KMgF_3$:Eu crystals with an Eu concentration of 0.01, 0.5, and 2.5 mol % at 10 K. (b) Extended spectra near site *A* in the spectral range of 569.8–570.5 nm.

Eu^{3+} can be formed by an Eu^{3+} ion with two vacancies located far from the Eu^{3+} ion. However, no cubic-site Eu^{3+} is produced in $KMgF_3$:Eu^{3+}, which seems to be due to the strong electrostatic attraction between Eu^{3+} and the vacancies unlikely to the cubic sites Eu^{2+} and Sm^{2+} produced in $KMgF_3$.[10,11,13] Eu^{2+} and Sm^{2+} in KCl, similarly to Eu^{3+} in $KMgF_3$, do not occupy a site with cubic symmetry but a site with C_{2V} or C_{4V} symmetry.[1,6]

In case of Ce^{3+}-doped $KMgF_3$ (Ref. 9) and CaF_2,[3] an increase of Ce^{3+} concentration causes significant growth of clustered sites. In Eu^{3+}-doped $KMgF_3$, the growth of the excitation line *B* relative to the line *A* on doping concentration (Fig. 4) is behavior typical of clustering. We thus attribute the site *A* to the isolated Eu^{3+}-V_c pairs, while the site *B* and other minority sites can be attributed to the sites due to the clustering of Eu^{3+}-V_c pairs. The clustering behavior of Eu^{3+} is similar to that of Ce^{3+} in $KMgF_3$.

The two charge-compensating vacancies have the same charge and so they repel each other. Therefore, the positions where the vacancies are favored lie on the opposite sites in terms of an Eu^{3+} ion giving a C_{4V} site symmetry of Eu^{3+}. However, the crystal-field symmetries of all the sites appearing in the excitation spectra are assumed to be lower than

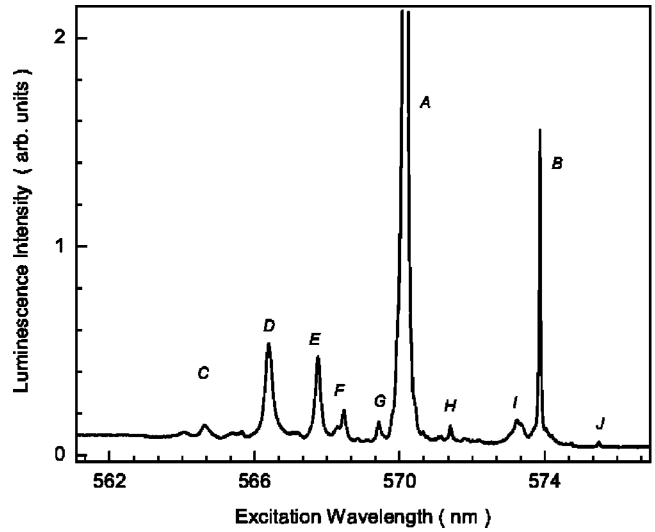

FIG. 5. Enlarged excitation spectrum for the ${}^7F_0 \rightarrow {}^5D_0$ transition of Eu^{3+} in the $KMgF_3$ crystal (sample II: Eu concentration of 0.05 mol %).

C_{4V}, as discussed above. The C_{4V} symmetry seems to be distorted by a defect center formed together with the Eu^{3+}-V_c pair. One possible defect center is an interstitial fluorine atom (H center) which enters the $KMgF_3$ lattice adjacent to the Eu^{3+}-V_c pair due to enough space created by two charge-compensating vacancies. It is known that the intrinsic interstitial fluorine atom (H center) exists adjacent to

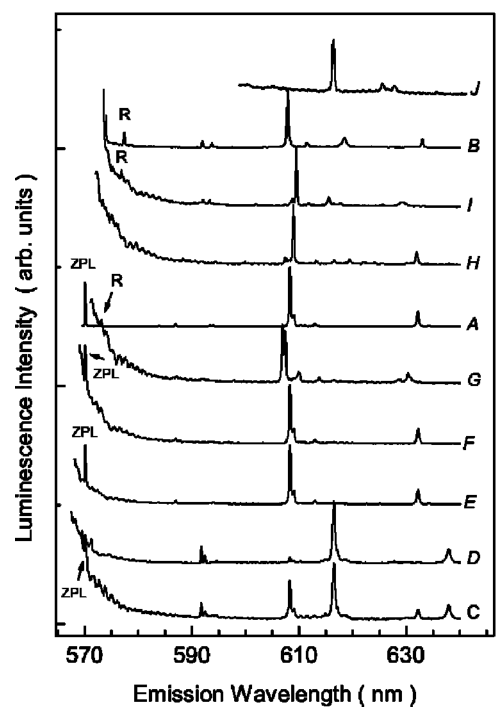

FIG. 6. Emission spectra for the ${}^5D_0 \rightarrow {}^7F_J$ (J=0,1,2) transitions of Eu^{3+} under the resonant site-selective excitations at 10 K. The excitation lines are indicated at the right side of the emission spectra. Intensities are normalized to the most intense ${}^5D_0 \rightarrow {}^7F_2$ peak. Zero phonon lines (ZPL) are designated in the spectra *A*, *F*, *E*, *D* and *C* at 570.16 nm. *R* denotes Raman line at 102 cm^{-1}.

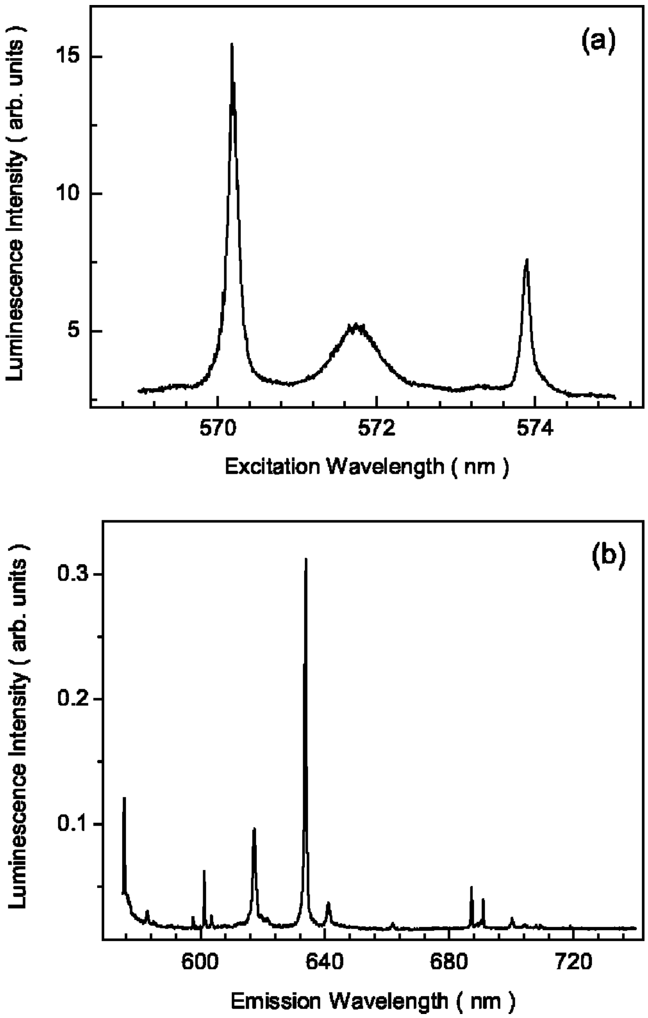

FIG. 7. (a) Excitation spectrum of the $^7F_0 \rightarrow {}^5D_0$ transition for the 355-nm-irradiated $KMgF_3$:Eu crystal at 10 K. (b) Emission spectrum of the $^5D_0 \rightarrow {}^7F_J$ transitions obtained by exciting at 571.7 nm appearing in (a).

impurity cation ions (Li^+, Na^+) whose ionic radii are smaller than the K^+ ions in $KMgF_3$.[25] The new site in the excitation spectrum (Fig. 9) obtained after 355-nm irradiation on the sample is evidence of the presence of interstitial fluorine atoms. The interstitial fluorine atom combines with a neighboring fluorine ion to form a molecular ion (F_2^-) by UV irradiation.[26,27] The F_2^- molecular ion perturbs the crystal field at the Eu^{3+} ion, resulting in the production of a new Eu^{3+} center.

Clustering occurs in various rare-earth-doped alkali-metal halides[1,2,4–6] and alkaline-earth halides.[3] The clustering state of rare-earth ions in host materials can be changed by thermal treatment, and its behavior depends on the host materials. Santiuste *et al.*[4] observed different types of EuX_2 (X =Cl, Br, or I) precipitates in Eu^{2+}-doped KCl in which the Eu^{2+} luminescence exhibits no temperature-dependent quenching in the range of 10–300 K, unlike Eu^{3+} luminescence in $KMgF_3$. The temperature-dependent quenching was reported for Sm^{2+} luminescence in KCl crystals by Guzzi *et al.*[28] and Ramponi *et al.*[1] All the Sm^{2+} centers exhibit quenching behavior at low temperatures in KCl:Sm^{2+}, and

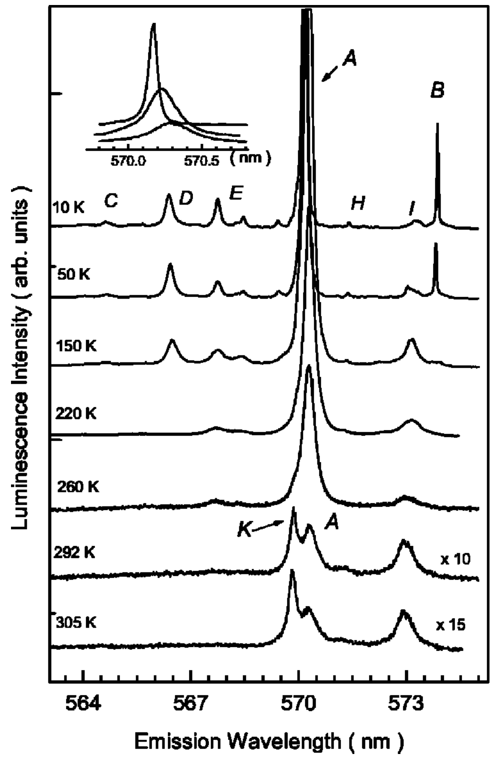

FIG. 8. Excitation spectra for the luminescence due to the $^5D_0 \rightarrow {}^7F_J$ (J=1,2,…,6) transitions measured at different temperatures. The temperatures are indicated at the left side of the spectra. The inset is the extended spectra near the site C in the spectral range 569.8–570.8 nm for 10, 150, and 220 K.

the luminescence even from the isolated Sm^{2+}-V_c pairs is quenched at 12 K.[1] Guzzi *et al.* explained the phenomena in terms of a nearby $4f^55d$ configuration which thermally depopulates the emitting $^5D_0$ level. In the case of Eu^{3+}, however, the nonradiative relaxation processes do not take place via the thermal population of the $4f^55d$ configuration even at room temperature because the $4f^5d$ configuration of Eu^{3+} lies at much higher energy with respect to the $^5D_0$ level.

The thermal quenching of the Eu^{3+} luminescence is ascribed to an energy transfer from Eu^{3+} to a defect center such as the H center in $KMgF_3$.[25–27] The clustering of Eu^{3+}-V_c pairs further enhances the energy transfer rate between Eu^{3+}

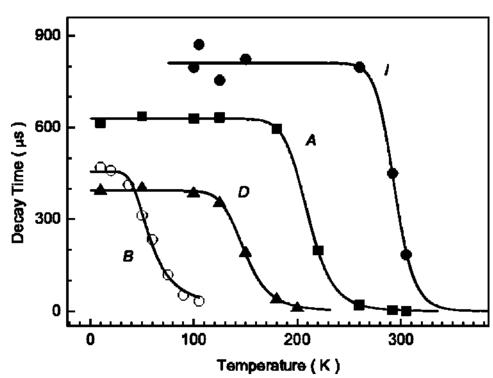

FIG. 9. Decay times for the sites A, B, D, and I as a function of temperature. Solid curves are fits to a three-level decay system.

ions to quench the luminescence at lower temperature in $KMgF_3:Eu^{3+}$. The excited Eu^{3+} ions due to the $^7F_0 \rightarrow {}^5D_0$ transitions may relax to the ground state by very rapid energy transfer among Eu^{3+} ions and finally return to the ground state by transferring their energy to the sink. As shown in Figs. 8 and 9, the thermal quenching tends to occur at lower temperatures for the sites with shorter lifetimes, except for the site K, which exhibits no quenching behavior up to 305 K.

The aggregation of rare-earth ions can be controlled by appropriate annealing and subsequent quenching procedures. The Sm^{2+} clusters in alkali-metal halides are dissolved in part by annealing and quenching processes (e.g., see Ref. 1). We took the annealing and quenching experiments on the samples under Ar-gas atmosphere to observe the change in clusters. However, no change in spectral features of all the sites was observed in the temperature range 10–305 K. The same behavior was reported in $KMgF_3:Ce^{3+}$ by Francini *et al.*, from which they ruled out the possibility of clustering of Ce^{3+} ions and argued that cubic-site Ce^{3+} ions are present. We suggest that the clustering of Eu^{3+} occurs in $KMgF_3$, although the clusters are not destroyed by annealing and quenching treatment, unlike those in $KCl:Sm^{2+}$. The Eu^{3+}-V_c pairs dissolved by annealing treatment may recombine with each other very rapidly or an association energy of the clusters is too large to be dissolved by a given thermal energy in $KMgF_3$. Ramponi *et al.*[1] reported that the annealing and quenching treatment does not completely dissolve the clusters even by very fast quenching for the annealed sample.

ACKNOWLEDGMENTS

This work was supported by Grant No. R05-2001-000-00134-0 from the Basic Research Program of the Korea Science & Engineering Foundation. One of the authors (T.T.) thanks the Japan Society for the Promotion of Science for partial support by the Grant-in-Aid for Science Research (C).

*Corresponding author. Email address: hjseo@pknu.ac.kr; Fax: 82-51-611-6357.

[1] A.J. Ramponi and J.C. Wright, Phys. Rev. B **31**, 3965 (1985).
[2] A.J. Ramponi and J.C. Wright, Phys. Rev. B **35**, 2413 (1987).
[3] S.W.S McKeever, M.D. Brown, R.J. Abbundi, H. Chan, and V.K. Mathur, J. Appl. Phys. **60**, 2505 (1986).
[4] J.E. Munoz Santiuste, J. Garcia Sole, and M. Manfredi, Phys. Rev. B **42**, 11 339 (1990).
[5] F.J. Lopez, H. Murrieta S., J. Hernandez A., and J. Rubio O., Phys. Rev. B **22**, 6428 (1980).
[6] F.M. Matinaga, L.A.O. Nunes, S.C. Zilio, and J.C. Castro, Phys. Rev. B **37**, 993 (1988).
[7] A. Gektin, V. Komar, V. Shlyahturov, and N. Shiran, IEEE Trans. Nucl. Sci. **43**, 1295 (1996).
[8] N.J.M. Le Masson, A.J.J. Bos, A.J.M. Winkelman, and C.W.E. van Eijk, IEEE Trans. Nucl. Sci. **48**, 1143 (2001).
[9] M. Martini, F. Meinardi, and A. Scacco, Chem. Phys. Lett. **293**, 43 (1998).
[10] H.J. Seo, B.K. Moon, and T. Tsuboi, Phys. Rev. B **62**, 12 688 (2000).
[11] W. Zhang, H.J. Seo, B.K. Moon, S.S. Yi, and K. Jang, J. Alloys Compd. **374**, 32 (2004).
[12] T. Tsuboi and A. Scacco, J. Phys.: Condens. Matter **10**, 7259 (1998).
[13] R. Francini, U.M. Grassano, M. Tomini, S. Boiko, G.G. Tarasov, and A. Scacco, Phys. Rev. B **55**, 7579 (1997).
[14] A. Ellens, A. Meijerink, and G. Blasse, J. Lumin. **59**, 293 (1994).
[15] M. Yamaga, M. Honda, N. Kawamata, T. Fujita, K. Shimamura, and T. Fukuda, J. Phys.: Condens. Matter **13**, 3461 (2001).
[16] I.R. Ibragimov, I.I. Fazlizhanov, M.L. Falin, and V.A. Ulanov, Sov. Phys. Solid State **34**, 1745 (1992).
[17] M.L. Falin, V.A. Latypov, B.N. Kazakov, A.M. Leushin, H. Bill, and D. Lovy, Phys. Rev. B **61**, 9441 (2000).
[18] R. Francini, U.M. Grassano, L. Landi, A. Scacco, M. D'Elena, M. Nikl, N. Cechova, and N. Zema, Phys. Rev. B **56**, 15 109 (1997).
[19] B.N. Kazakov, A.M. Leushin, G.M. Safiullin, and V.F. Bespalov, Phys. Solid State **40**, 1836 (1998).
[20] N.V. Shiran, V.K. Komar, V.V. Shlyakhturov, A.V. Gektin, and Y.A. Nesterenko, Radiat. Eff. Defects Solids **136**, 197 (1995).
[21] L.D. Merkle, Phys. Rev. B **42**, 3783 (1990).
[22] J.L. Sommerdijk and A. Bril, J. Lumin. **12/13**, 669 (1976).
[23] C. Gorller-Walrand and K. Binnemans, *Rationalization of Crystal-Field Parametrization*, in *Handbook on the Physics and Chemistry of Rare Earths*, edited by K.A. Gschneidner, Jr. and L. Eyring (North-Holland, Amsterdam, 1996), Vol. 23, Chap. 155.
[24] C. Gorller-Walrand, K. Binnemans, and L. Fluyt, J. Phys.: Condens. Matter **5**, 8359 (1993).
[25] B.H. Rose, J.E. Rhoads, and L.E. Halliburton, Phys. Rev. B **14**, 3583 (1976).
[26] J.E. Rhoads, B.H. Rose, and L.E. Halliburton, Phys. Rev. B **11**, 5115 (1975).
[27] J.T. Lewis, J.L. Kolopus, E. Sonder, and M.M. Abraham, Phys. Rev. B **7**, 810 (1973)
[28] M. Guzzi and G. Baldini, J. Lumin. **6**, 270 (1973).